

## **Distribution Agreement**

In presenting this thesis as a partial fulfillment of the requirements for a degree from Emory University, I hereby grant to Emory University and its agents the non-exclusive license to archive, make accessible, and display my thesis in whole or in part in all forms of media, now or hereafter now, including display on the World Wide Web. I understand that I may select some access restrictions as part of the online submission of this thesis. I retain all ownership rights to the copyright of the thesis. I also retain the right to use in future works (such as articles or books) all or part of this thesis.

Christina Xu

November 20, 2024

Modulation of Intramuscular Fat Remodeling by GDF10 in High-Fat Diet-Induced Obesity

by

Christina Xu

Hyojung Choo  
Adviser

Biology

Hyojung Choo

Adviser

Skye Comstra

Committee Member

Young Jang

Committee Member

2024

Modulation of Intramuscular Fat Remodeling by GDF10 in High-Fat Diet-Induced Obesity

By

Christina Xu

Hyojung Choo  
Adviser

An abstract of  
a thesis submitted to the Faculty of Emory College of Arts and Sciences  
of Emory University in partial fulfillment  
of the requirements of the degree of  
Bachelor of Science with Honors

Biology

2024

## Abstract

### Modulation of Intramuscular Fat Remodeling by GDF10 in High-Fat Diet-Induced Obesity By Christina Xu

Obesity is becoming an epidemic health concern, significantly impacting skeletal muscle health through increased fatty infiltration and weakened muscle strength. Our study investigates the effects of high fat diet (HFD)-induced obesity on muscle health, evaluating the fatty infiltration, neuromuscular connection, and muscle strength. One of the main contributors of intramuscular adipogenesis is fibro-adipogenic progenitors (FAPs), which differentiate into adipocytes or fibroblasts depending on different cytokine signaling. However, FAPs also express high level of growth differentiation factor 10 (GDF10) that is known to promote neuromuscular junction integrity and negatively correlated with the level of fat accumulation. Therefore, we target GDF10 to examine its potential therapeutic effect in mitigating obesity-induced muscle damages. Utilizing both tibialis anterior (TA) and tongue muscles from the mice models, we assessed the impact of GDF10 overexpression in reducing fat infiltration and preserving limb muscle function. Our results indicate that HFD significantly exacerbates fatty infiltration and NMJ denervation in muscle tissues, leading to the decline in muscle grip strength. GDF10 overexpression was found to reduce adipocyte size in both glycerol-injured TA and HFD-fed Tongue muscles, suggesting its role in inhibiting adipocyte hypertrophy in muscles. Our findings contribute to understanding the mechanisms of obesity-induced muscle remodeling and support further research into GDF10 as a potential intervention for maintaining muscle health in obese individuals.

Modulation of Intramuscular Fat Remodeling by GDF10 in High-Fat Diet-Induced Obesity

By

Christina Xu

Hyojung Choo  
Adviser

A thesis submitted to the Faculty of Emory College of Arts and Sciences  
of Emory University in partial fulfillment  
of the requirements of the degree of  
Bachelor of Science with Honors

Biology

2024

## Table of Contents

<b>Introduction .....</b>	<b>1</b>
<b>Materials and Methods .....</b>	<b>3</b>
<b>Result .....</b>	<b>7</b>
<b>Discussion.....</b>	<b>11</b>
<b>Reference .....</b>	<b>14</b>
<b>Figure Legends .....</b>	<b>16</b>
<b>Figures.....</b>	<b>19</b>

# Introduction

The rising prevalence of obesity has developed into a severe global health problem. From 2021 to 2023, both men and women adult obesity rate has increased to 40.3% in the US (Products - Data Briefs - Number 508 - September 2024). Moreover, the impact of obesity extends beyond pathological conditions and includes risks that directly impair bodily functions, particularly in muscle tissue. Specifically, obesity initiates cellular and molecular changes, causing fatty infiltration within the muscle tissue. The intermuscular adipose tissue (IMAT) generated by fatty infiltration increases susceptibility to injury, contributes to chronic inflammation by secreting adipokines(Shinohara et al.), and develops insulin resistance through the accumulation of diacylglycerol and acyl-CoA intermediates (van Herpen and Schrauwen-Hinderling), ultimately impairs muscle function and damages the metabolism. Therefore, it is critical to study the effects of obesity induced intramuscular adipogenesis and its impact on muscle strength. Further, we investigate potential therapeutic agents that inhibit and reverse the intramuscular adipogenesis caused by high-fat-diet induced obesity.

One of the main contributors of fatty infiltration in muscle is fibro-adipogenic progenitor cells (FAPs), muscle-resident mesenchymal stem cells that play a critical role in muscle repair and regeneration under healthy conditions (Joe et al.). However, upon chronic muscle injury, FAPs are differentiated into fibroblasts or adipocytes via the control of macrophage secreted cytokines, generating fibrosis or fat infiltration (Molina et al.). Specifically, muscle injury caused by glycerol injection can activate FAPs and induce their differentiation into perilipin<sup>+</sup> adipocytes (Norris et al.). Recently, studies have highlighted the new functions of FAPs in maintaining muscle mass by supporting neuromuscular junction (NMJ) interactions by the secretion of growth differentiation factor 10 (GDF10) (Uezumi et al.). Other studies found GDF10 promotes

axonal sprouting and enhances recovery following stroke, supporting neural-muscular connections (Li et al.). In addition to neural support, the expression of GDF10 is negatively correlated with the level of obesity. Studies had shown overexpressing GDF10 can inhibit adipocyte differentiation in liver (Platko et al.), plasma of obese children contains lower level of GDF10 (Yousof et al.), and inhibition of GDF10 stimulates adipogenesis in adipose tissue (Hino et al.). Based on the neural muscular support and negative role of GDF10 in adipogenesis, GDF10 may have the potential to protect muscles from intramuscular adipogenesis.

High-fat diet (HFD) is a major contributor to obesity. Thus, we employed HFD mouse models to investigate the extent of muscle damage caused by obesity and to evaluate the potential of GDF10 to rescue these damages. Specifically, we targeted the fatty infiltration in tibialis anterior (TA) muscle and tongue muscle. Mice have residential intramuscular adipocytes infiltrated in Tongue muscle but not in TA muscle, so we stimulated the FAPs differentiation to adipocytes in TA by glycerol injury.

In this study, we focus on the impact of a high-fat diet (HFD) on fatty skeletal muscle, specifically examining how fat infiltration is increased and how neuromuscular connection is changed. Additionally, we explore the potential of GDF10 as a therapeutic agent for reducing fat infiltration and preserving the neuromuscular integrity and function of both limb and tongue muscles. By investigating GDF10's effects on these muscle groups, we aim to determine whether it can mitigate obesity-induced damage, thereby offering insight into its application for improving muscle health in obese individuals.

# Materials and Methods

## Mice models

We used wild-type male mice (C57BL/10ScSnJ, purchased from Jackson Laboratory, Jax000476), which were prone to generate more fat compared to C57BL/6 at 12 weeks of age. After limb muscle injury, we fed mice a 40% high-fat diet (HFD, purchased from Bio-Serv) for one month. For tongue muscle experiment, we fed mice (8 weeks old) for 6 months with 40% HFD instead of injury due to high mortality risk of tongue muscle injury. To ensure the effect of HFD, we measured body weight weekly.

## In vivo muscle glycerol injury and GDF10 virus injection

We induced intramuscular adipogenesis in the limb muscles using a glycerol injury model (Mahdy), focusing on the tibialis anterior (TA) muscle. Mice were anesthetized with 3% isoflurane in a sealed chamber. To alleviate any potential discomfort, we administered 0.05 mg/kg of buprenorphine through subcutaneous injections for analgesia. We injected both TA muscles longitudinally with 25  $\mu$ l of a 50% glycerol in PBS solution using a syringe.

To observe the impact of overexpression of GDF10 in the glycerol-injured muscles. Three weeks after the glycerol injury, 10  $\mu$ l of AAV8-GDF10-RFP virus (1X10<sup>11</sup> GC) or control AAV8-RFP virus (1X10<sup>11</sup> GC) was injected into both TA muscles with the same injection protocol as glycerol injury. For tongue muscle, 10  $\mu$ l of AAV8-GDF10-RFP virus (1X10<sup>10</sup> GC) or control AAV8-RFP virus (1X10<sup>10</sup> GC) was injected into tongue muscles.

## Histology and immunofluorescence

To assess the effect of diet-induced obesity and FAPs ablation on muscle histology, we performed histological analysis focusing on adipocytes and neuromuscular junctions (NMJs) via immunofluorescence staining of dissected tibialis anterior (TA) and tongue muscles. The muscle

tissues were dissected and preserved by embedding them in molds filled with Tissue-Tek O.C.T. (Sakura Finetek, United States). Tissue freezing was achieved by placing the bottom of the molds in contact with the surface of 2-methylbutane, which was cooled with liquid nitrogen. The preserved samples were then stored at -80°C. Longitudinal tissue sections of 30  $\mu$ m thickness and cross-sectional tissue sections of 15  $\mu$ m were collected using a CryoStat NX50 Cryostat.

To visualize intramuscular adipocytes, we immunostained the longitudinal TA sections and cross-sectional Tongue base sections. Each section was fixed with 4% paraformaldehyde (PFA) for 10 minutes prior to immunostaining and washed with PBS three times each for five minutes. The fixed tissue sections were then incubated in blocking buffer (0.5% Triton X-100, 10% donkey serum, and 1% bovine serum albumin in PBS) for 1 hour at room temperature, followed by overnight incubation at 4°C with a 1:200 dilution of primary anti-Perilipin A/B antibody produced in rabbit (P1873-200UL, Sigma Aldrich) in 10% blocking buffer. The following day, sections were incubated with Alexa 594-conjugated Donkey anti-rabbit secondary antibody (1:200, Jackson ImmunoResearch) for 1 hour at room temperature. Cell nuclei were stained with 4',6-diamidino-2-phenylindole (DAPI) (1  $\mu$ g/ml) for 3 minutes at room temperature. The slides were then mounted with Vectashield (Vector Laboratories).

For NMJ integrity evaluation, nerve terminals were immunostained by incubating tissue sections with Anti-Neurofilament heavy polypeptide antibody (ab8135, Abcam) overnight at 4°C, followed by a 1-hour room temperature incubation with FITC-conjugated anti-rabbit antibody (1:200). Motor end plates were stained with alpha-bungarotoxin (Molecular Probes  $\alpha$ -Bungarotoxin, Alexa Fluor 594 Conjugate, Thermo Fisher) for 30 minutes. The sections were then mounted with Vectorshield.

Immunofluorescent images were captured using a Nikon microscope at 10 X magnification for perilipin images and 20 X for NMJ images. Images were analyzed manually using ImageJ. Adipocyte count and size in perilipin-stained images were measured by tracing individual cells. For rigor, at least one hundred NMJ markers were identified and counted per sample. NMJ integrity was quantified by calculating the percentage of denervated to total NMJs. NMJ denervation was identified by the absence of nerve terminals while the corresponding motor end plate was in place. A complete overlap of the two signals indicated an innervated NMJ while the loss of a partial motor end plate indicates partial innervation.

### **Muscle Grip Strength**

The muscle grip strength of each mouse was measured two days before dissection to assess the effect of the treatment on muscle function. Hindlimb strength was determined by subtracting the average forelimb strength force from the average full-limb strength force. We obtained a minimum of seven valid grip strength values for each measurement method.

For the forelimb measurement, a T-shaped grip bar was attached to the grip strength meter, which was set up perpendicular to the floor. The mouse could grip the bar with its forepaws while keeping its torso perpendicular to the floor. Mice were pulled downward to ensure it maintained a firm grip with both forepaws. The grip strength meter recorded the maximal grip strength. For the combined forelimb, a 4x6 grid was attached to the grip strength meter, allowing the mouse to grip the grid with four limbs while keeping its torso perpendicular to the floor. The tail was gently pulled downward, with the force gradually increasing. A valid measurement was achieved by maintaining this pulling force for a few seconds, ensuring the mouse maintained a firm grip on the grid. The meter recorded the maximum force.

### **Statistical analyses**

Statistical analysis was performed using GraphPad Prism version 9.0 for 64-bit Windows. The statistical methods, ranges of p values, and sample size are indicated in the figure legends. For all experiments, results are expressed as the mean  $\pm$  standard error of the mean (SEM). The statistical difference was determined by unpaired student's t-test, 1-way ANOVA, or 2-way ANOVA if the data was normally distributed determined by normality test (Shapiro-Wilk test and Kolmogorov-Smirnov test).  $p<0.05$  was considered statistically significant.

# Result

## HFD induced obesity disrupts limb muscle integrity and functionality

To investigate the impact of HFD-induced obesity on limb muscle, we induced intramuscular adipogenesis by injecting glycerol into the TA muscles of mice and feeding them with HFD for one month while monitoring their body weight (Figure 1A). To evaluate muscle functionality after HFD, we measured hindlimb grip strength 28 days post glycerol injury. We observed a 1.4 times reduction in hindlimb force in HFD-fed mice compared to normal diet (ND)-fed mice with glycerol injury. However, no difference between ND-fed uninjured and injured groups was confirmed indicating fully recovered muscles after glycerol injury in ND-fed mice (Figure 1B).

Since muscle weakness has been found to be associated with intramuscular adipocyte deposition (Norris et al.) and NMJ denervation (Gonzalez-Freire et al.), we aimed to explore the impact of HFD-induced obesity on muscle function, intramuscular adipogenesis and NMJ integrity in glycerol-injured TA muscles.

To assess the impact of HFD on intramuscular adipogenesis, we performed immunofluorescence staining for perilipin 1, which is expressed on the surface layer of intracellular lipid droplets in adipocytes, on longitudinal TA sections. The staining showed dense, thick layers of intramuscular adipose tissue in obese mice, contrasting with the dispersed adipocytes observed in ND-fed controls (Figure 1C). Upon quantitative analysis, HFD-fed mice express 4.7 times higher in the ratio of adipocyte area to the muscle area (Figure 1D). We confirmed that both adipocyte hyperplasia (Figure 1E) and hypertrophy (Figure 1F) contribute to the increase in overall adipocyte area of HFD-fed mice.

Additionally, we analyzed NMJ integrity by sorting and counting the number of denervated, innervated, and partially innervated NMJs via immunofluorescence staining. Innervation was determined by the complete overlap of neurofilament and acetylcholine receptors, and denervation was determined by the complete absence of neurofilament (Figure 1G). The denervation rate of HFD-fed mice is around three times higher than ND-fed mice (Figure 1H and 1I). This indicates that HFD not only promotes adipogenesis but also impairs neuromuscular integrity, potentially exacerbating muscle dysfunction in obesity.

**HFD induced obesity aggravates intramuscular adipogenesis and NMJ denervation in tongue muscle.**

To further validate the effects of a high-fat diet (HFD) on intramuscular adipogenesis, we examined the tongue muscle, which, unlike the TA muscle, naturally has resident adipocytes infiltrated between the myofibers. We treated the mice with HFD for 3 months and 6 months to observe the long-term effects of HFD-induced obesity. Starting at 2 months of age, mice were fed with HFD for either 3 or 6 months, with body weight measured monthly. A significant increase in body weight was observed in HFD-fed mice as early as one month into the diet (Figure 2A).

To evaluate the impact on intramuscular adipocytes, we quantified the size and number of adipocytes in cross-sections of the Tongue muscle. Mice on both 3-month and 6-month HFD treatments showed a significant increase in the percentage of adipocyte area and average adipocyte size compared to mice fed a normal diet (ND) (Figure 2B and 2D). Interestingly, the number of adipocytes did not differ significantly between HFD and ND groups (Figure 2C). Additionally, while there was no difference in adipocyte area between the 3-month and 6-month HFD groups, the ND-fed mice displayed a significant increase in adipocyte area with age, as

expected, since the 6-month group had more time to grow and accumulate fat (Figure 2B and 2D). To examine the long-term effects of HFD, we focused on mice that had been on HFD for 6 months in subsequent experiments.

To assess the impact of HFD on neuromuscular junction (NMJ) integrity, we analyzed longitudinal sections of the Tongue muscle and focused on the NMJs within the genioglossus (GG) muscle. Both male and female Tongue mice were included in the analysis, with both showing a threefold increase in denervated NMJs in HFD-fed mice compared to ND-fed controls. However, male mice exhibited a higher trend of NMJ denervation, so we chose to focus on male mice in the following experiments.

### **GDF10 overexpression promotes muscle strength and attenuates intramuscular adiposity in HFD-fed mice.**

Previous studies have found overexpression of GDF10 can inhibit adipogenesis in adipose tissues and liver (Platko et al.), and that the inhibition of GDF10 leads to increased adipogenesis (Camps et al.; Hino et al.). In our study, we focused on fat-infiltrated TA muscle to assess whether GDF10 has the potential to protect the muscle against fatty infiltration. HFD-fed mice received control or GDF10 virus injections two weeks after glycerol-induced injury, and their body weight was monitored weekly. (Figure 3A). Mice injected with GDF10 virus showed lower growth in body weight than the control virus injected mice starting a week after the virus injection (Figure 3A). The GDF10 expression level was confirmed by qPCR, showing high levels of GDF10 RNA in the injected muscle (Figure 3B). Four weeks after virus injection, hindlimb muscle grip strength was measured to evaluate the injured muscle function. We found stronger grip strength in the GDF10 virus injected group compared to the control (Figure 3C). Perilipin 1 staining revealed a reduced total adipocyte area in the GDF10 virus-infected region

(Figure 3D), mainly attributable to adipocyte hypotrophy (Figure 3F). Although there was no significant difference between the number of adipocytes from control virus and GDF10 virus injected mice, the number of adipocytes had a decreasing trend in the GDF10 virus injected mice (Figure 3E). Overall, the overexpression of GDF10 in TA muscle protects the muscle by regaining muscle grip strength and preventing intramuscular adipogenesis.

**GDF10 virus injection induced GDF10 overexpression alleviated adipogenesis in the tongues of high-fat diet (HFD)-induced obese mice.**

We also assessed the impact of GDF10 overexpression in the adipocyte infiltrated Tongue muscle to see the potential rescuing effect of GDF10. Throughout the 6-month HFD treatment, there were no significant differences in body weight between the GDF10 virus-injected group and the control virus-injected group (Figure 4A), indicating that GDF10 overexpression did not directly influence overall weight gain in these mice. Overexpression of GDF10 mRNA was successfully validated by qPCR, showing a significant increase in GDF10 expression in Tongue muscles compared to controls (Figure 4B). GDF10 overexpression had a noticeable impact on intramuscular adipogenesis. Specifically, injection of the GDF10 virus significantly reduced the size of adipocytes in the Tongue muscle (Figure 4C and E). While there was a trend toward a reduced number of adipocytes in the GDF10 group compared to the control, the difference was not statistically significant. This suggests that GDF10 may play a role in modulating adipocyte size. However, we did not find significant difference between the NMJ denervation rate of the control and GDF10 virus injected Tongue, but the control virus injected Tongue showed two times higher denervation rate than the no virus injected Tongue, suggesting this high denervation rate was caused by the viral infection in the muscle (Figure 4F).

## Discussion

Our study investigated the impact of HFD-induced obesity on skeletal muscle health, with a particular focus on intramuscular adipogenesis, NMJ integrity, and muscle grip strength. We also explored the potential of GDF10 overexpression as a therapeutic intervention to mitigate the detrimental effects of HFD-induced obesity by preventing and reducing fat infiltration in both Tongue and glycerol-injured TA muscles.

Under a HFD treatment, the mice showed more severe fatty infiltration and NMJ denervation in both the TA and Tongue muscles, while the hindlimbs grip strength was also reduced due to the HFD-induced obesity. Meanwhile, GDF10 virus induced overexpression showed the potential for inhibiting adipocyte growth by reducing the size of adipocytes in glycerol injured TA muscle and reducing both number and size of adipocytes in Tongue from mice fed with HFD for 6 months. This reduction suggests that GDF10 may influence the lipid metabolism of adipocytes, potentially limiting the lipid accumulation within the muscle. In TA muscle, there was a trend toward a decrease in the number of adipocytes with GDF10 overexpression, but the difference was not statistically significant (Figure 3E). This effect can be more observable if more samples were included in the study. Additionally, the GDF10 overexpression restored muscle grip strength in the mice with glycerol injured TA, suggesting the potential of GDF10 in maintaining muscle function and preventing the harm of HFD-induced obesity on force generation.

However, our study did not demonstrate a significant effect of GDF10 on NMJ integrity under HFD conditions (Figure 4F). While GDF10 is known to support neuromuscular connections in age-related sarcopenia (Uezumi et al.), our data may be insufficient to prove GDF10's counteracting effect against the NMJ damage caused by chronic obesity. Compared with the denervation rate in Tongue muscles without virus injection, both control virus and GDF10 virus-

injected Tongue muscles exhibited abnormally high denervation rates, suggesting that this abnormality may be driven by factors, such as viral infection, other than GDF10.

One limitation of our study is the methodological difference in virus injection between the TA and Tongue muscles. We found GDF10 virus injection causing a reduction in the body weight in mice with glycerol-injured TA (Figure 3A) but the body weight remained similar growth trend between GDF10 virus injected Tongue mice (Figure 4A). In case of TA muscle injection, we penetrated the muscle to thoroughly disperse the virus, leading to bleeding and likely systemic circulation of the virus. This could explain the observed decrease in body weight in TA-injected mice, as opposed to Tongue-injected mice, where the GDF10 virus effects remained localized to the GG muscle. This potential systemic effect in the TA group may have influenced the body weight trend of the glycerol injured, complicating the interpretation of the GDF10's localized effects.

Our findings suggest that targeting adipogenesis in skeletal muscle could be a promising strategy for improving muscle health in obese individuals. The reduction in adipocyte size with GDF10 overexpression highlights its potential as a therapeutic agent to mitigate the damaging effects of obesity on muscle function. The high NMJ denervation rate in virus injected group suggested the potential damaging effects caused by virus injection (Figure 4F). Thus, future studies can aim at altering the dosage of virus injection into the muscle, determining the optimal GDF10 virus dosage that is safe for preserving NMJ integrity. Additionally, our research has focused on animal models, but the translation of these findings to human conditions remains unclear. Investigating this connection of GDF10 expression and obesity in human sample can provide crucial insights into the relevance of GDF10 as a therapeutic target for obesity-related muscle degeneration in human populations.

Overall, our study provides new insights into the effects of HFD-induced obesity on skeletal muscle and highlights the potential of GDF10 to counteract some of the adverse outcomes associated with obesity-induced muscle damage. These findings lay the groundwork for future research aimed at developing targeted therapies to preserve muscle health in obese populations.

## Reference

Camps, Jordi, et al. "Interstitial Cell Remodeling Promotes Aberrant Adipogenesis in Dystrophic Muscles." *Cell Reports*, vol. 31, no. 5, May 2020. [www.cell.com](http://www.cell.com), <https://doi.org/10.1016/j.celrep.2020.107597>.

Gonzalez-Freire, Marta, et al. "The Neuromuscular Junction: Aging at the Crossroad between Nerves and Muscle." *Frontiers in Aging Neuroscience*, vol. 6, Aug. 2014. *Frontiers*, <https://doi.org/10.3389/fnagi.2014.00208>.

Hino, J., et al. "Bone Morphogenetic Protein-3b (BMP-3b) Is Expressed in Adipocytes and Inhibits Adipogenesis as a Unique Complex." *International Journal of Obesity*, vol. 36, no. 5, May 2012, pp. 725–34. [www.nature.com](http://www.nature.com), <https://doi.org/10.1038/ijo.2011.124>.

Joe, Aaron W. B., et al. "Muscle Injury Activates Resident Fibro/Adipogenic Progenitors That Facilitate Myogenesis." *Nature Cell Biology*, vol. 12, no. 2, Feb. 2010, pp. 153–63. [www.nature.com](http://www.nature.com), <https://doi.org/10.1038/ncb2015>.

Li, S., et al. "GDF10 Is a Signal for Axonal Sprouting and Functional Recovery after Stroke." *Nature Neuroscience*, vol. 18, no. 12, Oct. 2015, p. 1737. [pmc.ncbi.nlm.nih.gov](http://pmc.ncbi.nlm.nih.gov), <https://doi.org/10.1038/nn.4146>.

Mahdy, Mohamed A. A. "Glycerol-Induced Injury as a New Model of Muscle Regeneration." *Cell and Tissue Research*, vol. 374, no. 2, Nov. 2018, pp. 233–41. *PubMed*, <https://doi.org/10.1007/s00441-018-2846-6>.

Molina, Thomas, et al. "Fibro-Adipogenic Progenitors in Skeletal Muscle Homeostasis, Regeneration and Diseases." *Open Biology*, vol. 11, no. 12, Dec. 2021, p. 210110. [pmc.ncbi.nlm.nih.gov](http://pmc.ncbi.nlm.nih.gov), <https://doi.org/10.1098/rsob.210110>.

Norris, Alessandra M., et al. "Studying Intramuscular Fat Deposition and Muscle Regeneration: Insights from a Comparative Analysis of Mouse Strains, Injury Models, and Sex Differences." *Skeletal Muscle*, vol. 14, no. 1, May 2024, p. 12. *BioMed Central*, <https://doi.org/10.1186/s13395-024-00344-4>.

Platko, Khrystyna, et al. "GDF10 Blocks Hepatic PPAR $\gamma$  Activation to Protect against Diet-Induced Liver Injury." *Molecular Metabolism*, vol. 27, June 2019, p. 62. *pmc.ncbi.nlm.nih.gov*, <https://doi.org/10.1016/j.molmet.2019.06.021>.

Shinohara, Issei, et al. "Influence of Adiponectin and Inflammatory Cytokines in Fatty Degenerative Atrophic Muscle." *Scientific Reports*, vol. 12, no. 1, Jan. 2022, p. 1557. [www.nature.com](https://www.nature.com), <https://doi.org/10.1038/s41598-022-05608-x>.

Uezumi, Akiyoshi, et al. "Mesenchymal Bmp3b Expression Maintains Skeletal Muscle Integrity and Decreases in Age-Related Sarcopenia." *The Journal of Clinical Investigation*, vol. 131, no. 1, Jan. 2021, p. e139617. *pmc.ncbi.nlm.nih.gov*, <https://doi.org/10.1172/JCI139617>.

van Herpen, N. A., and V. B. Schrauwen-Hinderling. "Lipid Accumulation in Non-Adipose Tissue and Lipotoxicity." *Physiology & Behavior*, vol. 94, no. 2, May 2008, pp. 231–41. *ScienceDirect*, <https://doi.org/10.1016/j.physbeh.2007.11.049>.

Yousof, Tamana R., et al. "Reduced Plasma GDF10 Levels Are Positively Associated with Cholesterol Impairment and Childhood Obesity." *Scientific Reports*, vol. 14, no. 1, Jan. 2024, p. 1805. [www.nature.com](https://www.nature.com), <https://doi.org/10.1038/s41598-024-51635-1>.

## Figure Legends

### Figure 1. HFD-induced obesity disrupted the glycerol-injured TA muscle integrity and functionality

(A) Body weight trend of ND (n=5) and HFD (n=5) fed mice after glycerol injection. TA muscle was collected 4 weeks post-injury. Data were analyzed by 2-way ANOVA. (B) Hind limb grip strength of uninjured WT (n=5), glycerol-injured ND (n=5), and HFD (n=5). Data are normalized by dividing grip strength by body weight. Data were analyzed by 1-way ANOVA.

(C) Representative images of longitudinal immunostained TA sections of ND (bottom panels) and HFD-fed mice (top panels) stained for perilipin 1. The panels on the right are zoomed-in images of the boxed regions in the left panels. Original image scale bar = 1 mm. Zoomed-in images scale bar = 500  $\mu$ m (D-F) Quantification of adipocyte number and size in glycerol-injected TA muscles. Adipocytes from ND-fed mice (n=5) and HFD-fed mice (n=5) were circled, and areas were measured. The % adipocyte area was calculated by dividing the total adipocyte area by the total muscle area. (D) % adipocyte area. (E) Adipocyte number. (F) Average size of a single adipocyte. (G) Representative images of longitudinal TA immunofluorescence staining for NMJ: neurofilament (FITC) and acetylcholine receptor (TRITC) stained by antibody and  $\alpha$ -Bungarotoxin ( $\alpha$ BTX). Innervation is determined by complete overlap of neurofilament and motor end plate (top panel). Partial innervation is determined by partial absence of neurofilament (middle panel), and complete denervation is determined by complete absence of neurofilament (bottom panel). Scale bar = 20  $\mu$ m (H) Ratio of denervated, partially denervated, and innervated NMJ in ND and HFD-fed mice. A total of 339 NMJs were counted for ND-fed mice (n=3), and 315 NMJs were counted for HFD-fed mice (n=3). (I) Quantitative analysis of complete denervation rate between ND and HFD-fed mice.

Statistical significance was determined by Student T test (D, E, F, I). The value of all graphs represents mean  $\pm$  SEM.

**Figure 2. High-Fat Diet Exacerbates Adiposity and NMJ Degeneration in the Tongue Muscle**

(A) Body weight trends over six months of HFD (red, n=4) versus ND (black, n=4) feeding. Weight was monitored monthly. Data were analyzed using 2-way ANOVA. \*\*\*p < 0.001 and \*\*\*\*p < 0.0001 indicate significant differences between groups. (B-D) Quantitative analysis of adipogenesis level in cross-sectioned tongue muscle of ND and HFD-fed mice at 3 and 6 months. n=6 for each group. (B) Percentage of adipocyte area relative to total tissue area. (C) Number of adipocytes. (D) Average adipocyte size. Data were analyzed using Student's T-test. (E) Representative image of longitudinally sectioned tongue stained by Hematoxylin and Eosin (H&E). NMJ expression was observed in the GG muscle, circled in white. Scale bar = 1.5 mm. (F) Percentage of innervated, partially denervated, and fully denervated NMJs in male and female mice fed with 6 month of ND and HFD. A minimum of 300 NMJs were analyzed for each group (n=3). (G) Quantitative analysis of NMJ denervation rates between ND and HFD-fed male and female mice groups. n=3 for each group. Statistical significance was determined by Student T test (B, C, D, G). All data are shown as mean  $\pm$  SEM, with statistical significance noted by p-values above the horizontal line.

**Figure 3. GDF10 overexpression enhances muscle strength and reduces adipogenesis in TA of HFD-induced obese mice**

(A) Body weight progression in mice injected with control virus (black) or GDF10 virus (red) at the TA muscle two weeks after glycerol injury. Mice were monitored weekly for five weeks.

Data were analyzed by 2-way ANOVA. \* $p<0.05$  and \*\* $p < 0.01$  indicate significant differences between groups. (B) Relative GDF10 mRNA expression in the TA muscle for control and GDF10 virus-treated mice, assessed by qPCR. (C) Hind limb grip strength normalized by body weight for control and GDF10 virus-treated mice. (D-F) Quantitative assessment of intramuscular adiposity. (D) Percentage of total adipocyte area in TA muscle longitudinal sections. (E) Total number of adipocytes per tissue section. (F) Average size of individual adipocytes. Statistical significance was determined by Student T test (B-F). All data are presented as mean  $\pm$  SEM, with statistical significance indicated by p-values labeled above the horizontal line.

**Figure 4. GDF10 virus injection induced GDF10 overexpression alleviated adipogenesis in the Tongue of high-fat diet (HFD)-induced obese mice.**

(A) Body weight of control virus injected (n=4) and GDF10 virus injected (n=4) mice throughout six months of diet treatment. The virus was injected one month before tissue collection. (B) Relative mRNA expression level of GDF10 in Tongue muscle injected with control virus (n=3) and GDF10 virus (n=3). Area percentage (C), average area (D), and number (E) of adipocyte between control virus injected (n=4) and GDF10 virus injected (n=3) cross-sectioned tongues. (F) Quantitative analysis of NMJ denervation rates of Tongue muscles between control virus and GDF10 virus injected mice groups. n=3 for each group. Statistical significance was determined by Student T test (B, C, D, E). The value of all graphs represents mean  $\pm$  SEM, with statistical significance noted by p-values above the horizontal line.

# Figures

**Figure 1. HFD-induced obesity disrupted the glycerol-injured TA muscle integrity and functionality**

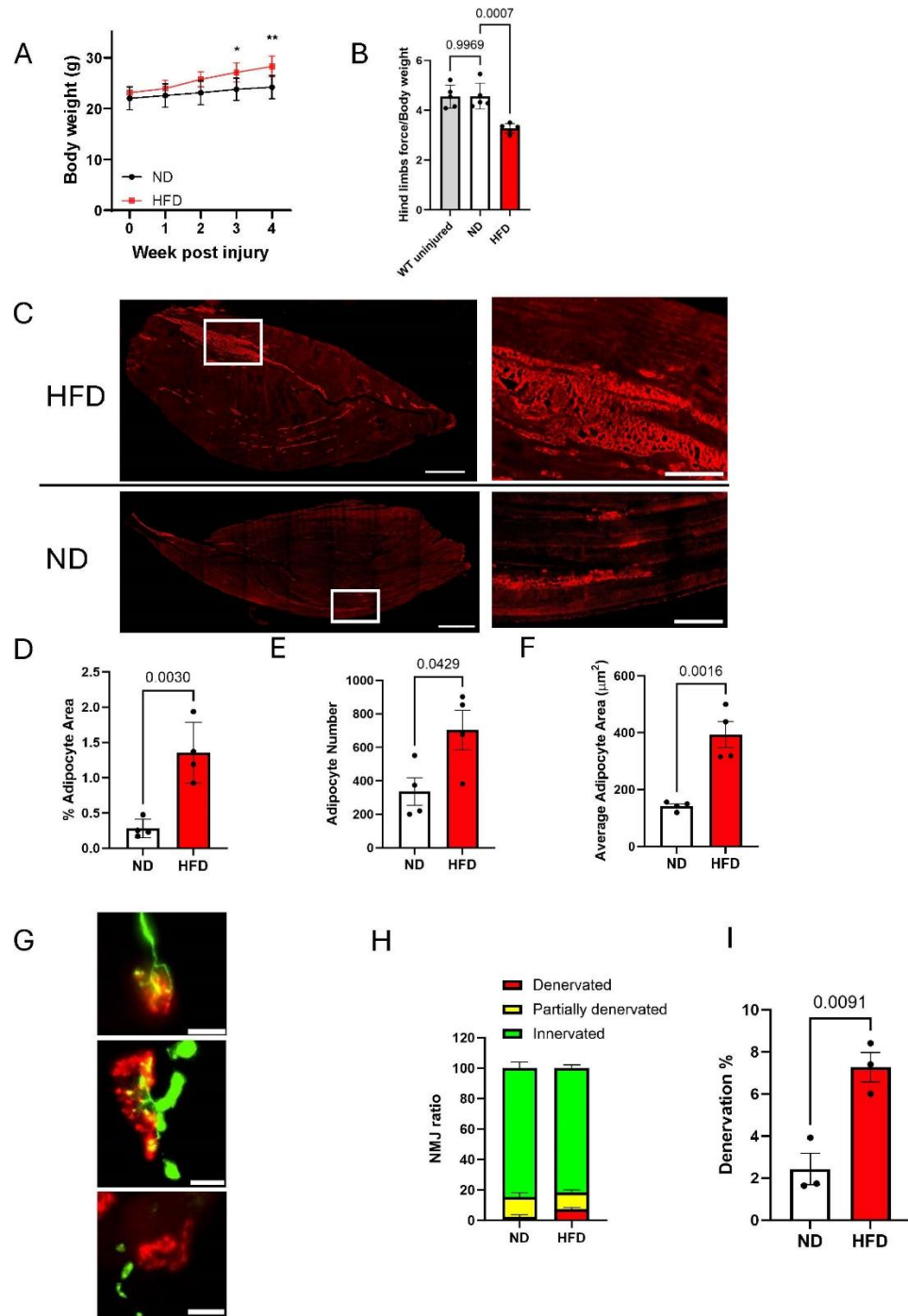


**Figure 2. High-Fat Diet Exacerbates Adiposity and NMJ Degeneration in the Tongue Muscle**

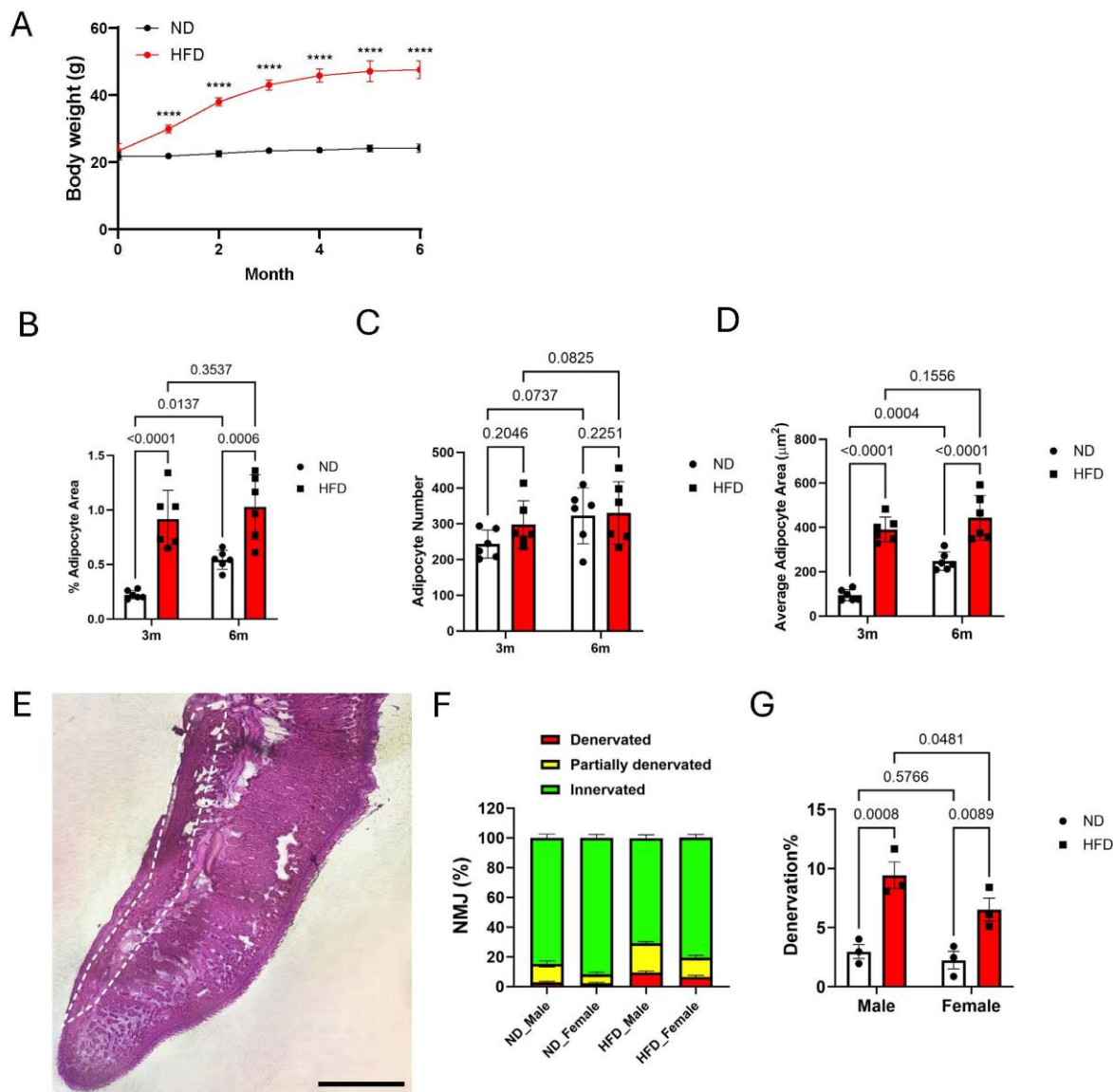


**Figure 3. GDF10 overexpression enhances muscle strength and reduces adipogenesis in HFD-induced obese mice**

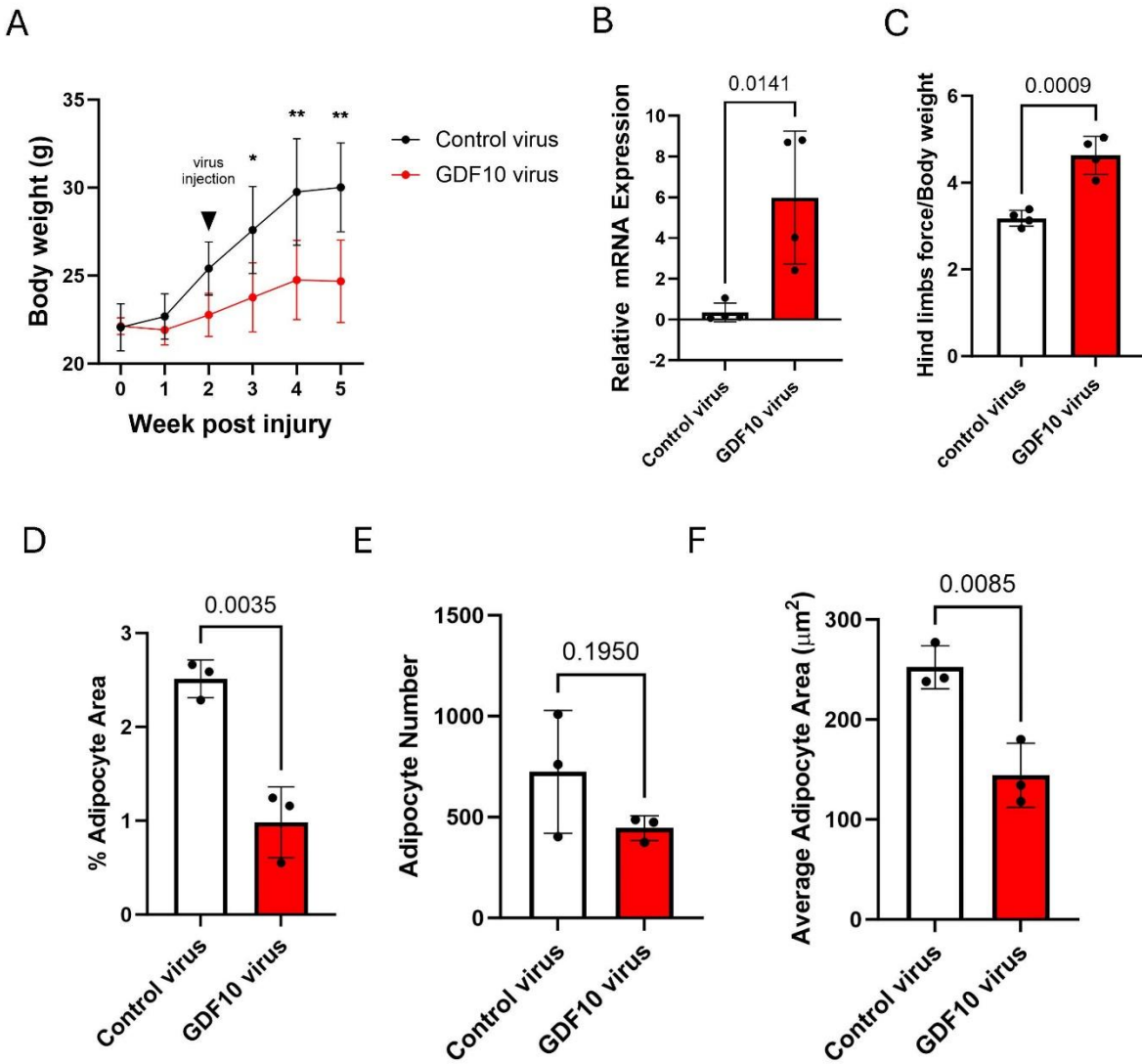


**Figure 4. GDF10 virus injection induced GDF10 overexpression alleviated adipogenesis in the tongues of high-fat diet (HFD)-induced obese mice.**

